

Waveguide quantum electrodynamics: Controllable channel from quantum interferenceQiong Li (李琼)^{1,2}, Lan Zhou (周兰)³, and C. P. Sun (孙昌璞)^{4,*}¹*State Key Laboratory of Theoretical Physics, Institute of Theoretical Physics, University of Chinese Academy of Science, Beijing 100190, China*²*Synergetic Innovation Center of Quantum Information and Quantum Physics, University of Science and Technology of China, Hefei, Anhui 230026, China*³*Department of Physics, Hunan Normal University, Changsha 410081, China*⁴*Beijing Computational Science Research Center, Beijing 100084, China*

(Received 28 August 2013; revised manuscript received 4 April 2014; published 13 June 2014)

We study a waveguide QED system with a rectangular waveguide and a two-level system inside, where the transverse magnetic TM_{mn} modes define the quantum channels of guided photons. It is discovered that the loss of photons from the TM_{11} channel into the others can be overcome by replacing it with a certain coherent superposition of TM_{mn} channels, which is named the controllable channel (CC), as the photons in the CC can be perfectly reflected or transmitted by the two-level system and never lost into the other channels. A dark state emerges when the photon is incident from one of the scattering-free channels orthogonal to the CC. The underlying physics mechanism is the multichannel interference associated with Fano resonance.

DOI: [10.1103/PhysRevA.89.063810](https://doi.org/10.1103/PhysRevA.89.063810)

PACS number(s): 42.50.Gy, 03.65.Nk, 42.50.Ct

I. INTRODUCTION

In a fully quantum network based on single-photon carriers to process quantum information, the essential task is to coherently control photon propagation by a local quantum node [1–5]. To this end, a hybrid system consisting of a one-dimensional (1D) waveguide coupled to a two-level system (TLS) has been extensively studied for physical implementation of the quantum node acting as a quantum switch [6–11] or a single-photon transistor [12,13]. This functional hybrid system can be realized in circuit-QED systems [14–18]. Inspired by its potential application in quantum computation and quantum information processing, the waveguide-QED system [19] has been studied intensively. The working principle of the quantum devices mentioned is based on the following observation: a single photon propagating in a 1D waveguide will be completely reflected if it is resonant with the transition frequency of the TLS (this is the Fano resonance phenomenon [6,20,21]).

This observation is made for a 1D waveguide without a cross section. However, a realistic waveguide of a finite cross section necessarily possesses transverse modes. Thus, photons guided in a realistic waveguide may be in different quantum channels defined by transverse modes. Each transverse mode has a cutoff frequency for the corresponding guiding mode. To demonstrate multichannel effects on single-photon scattering, Ref. [22] used the two-mode approximation with a quadratic dispersion relation and showed that a guided photon can be lost from one mode to the other. As a result, the total reflection on Fano resonance desirable in quantum devices cannot be well achieved. In order to overcome such multichannel loss, we revisit the waveguide QED by considering a realistic hybrid system without any overapproximation.

In this article, we study single-photon scattering by a TLS locally embedded in a waveguide of a finite rectangular cross section. In our approach, both the real dispersion relation and

multichannel effects are exactly taken into account. As for the multichannel-induced loss, we find that there exists a unique controllable channel (CC) defined by a particular superposition of the transverse magnetic TM_{mn} modes, in which the guided photons are lossless and thus well controlled by the TLS, since the complementary channels orthogonal to the CC are all decoupled from the TLS. The scattering-free channels (SFCs) are actually dark states to support the electromagnetically induced transparency. The CC and all SFCs make up the whole single-excitation Hilbert space of the waveguide-QED system. For a single photon confined in the CC, the Fano interference [20,21] between the incident wave and the re-emitted wave makes it totally reflected on resonance and well transmitted off resonance. Therefore, in a realistic waveguide the TLS can also work well, provided we use the CC to guide photons.

This paper is organized as follows: In Sec. II, we describe the model. In Sec. III, we present the scattering equation. In Sec. IV, we study single-channel scattering and its loss. In Sec. V, we study multichannel quantum interference and the CC. In Sec. VI, conclusions are summarized.

II. MODEL SETUP

We consider a waveguide of rectangular cross section with area $A = ab$, as shown in Fig. 1(a). The guiding modes in such a realistic waveguide are labeled (m,n,k) , with (m,n) the TM_{mn} mode (standing wave numbers in the cross section are $k_x = m\pi/a$, $k_y = n\pi/b$) and k the propagating wave number along the z direction. Each transverse mode (m,n) has the cutoff frequency $\Omega_{mn} = \sqrt{(m\pi/a)^2 + (n\pi/b)^2}$ (the unit $\hbar = 1 = c$ is used). According to the ascending order of the cutoff frequencies, we replace (m,n) with its sequence number j ; that is, $j = 1, 2, 3, \dots$ denote TM_{11} , TM_{31} , TM_{13} , \dots , respectively. The dispersion relation of the guiding modes is given by $\omega_{j,k} = \sqrt{\Omega_j^2 + k^2}$, as plotted in Fig. 1(c). The TLS of the transition frequency ω_a is located at $\mathbf{r}_a = (a/2, b/2, 0)$, whose ground (excited) state is denoted $|g\rangle$ ($|e\rangle$). The dipole oriented along the z direction couples the TM electric field. The total Hamiltonian $H = H_0 + V_r + V_d$ of the hybrid system is

*cpsun@csrc.ac.cn; <http://www.csrc.ac.cn/~suncp>

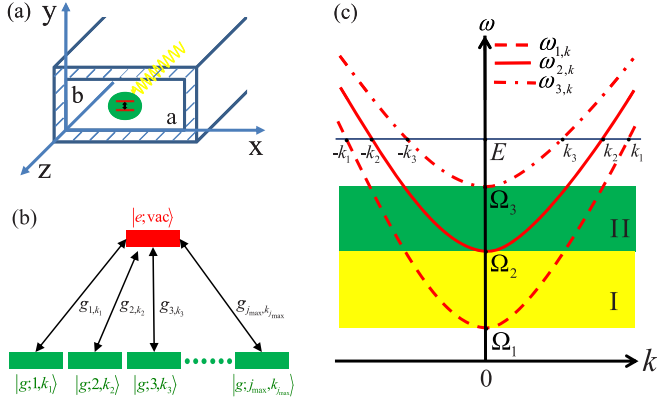


FIG. 1. (Color online) (a) Rectangular waveguide with a TLS located in the center of the cross section. The TLS is dipole-coupled to the TM guiding modes of the waveguide. $a = 2b$. (b) Schematic of the TLS as a multicomponent dark state. (c) Dispersion relation of the TM guiding modes of the waveguide. $\Omega_1 = 2.23607$, $\Omega_2 = 3.60555$, $\Omega_3 = 6.08276$. The frequency is in units of π/a . A photon with energy $E > \Omega_3$ can propagate in different modes with wave number $k = k_1, k_2, k_3$, etc.

given by the free part,

$$H_0 = \sum_j \int_{-\infty}^{+\infty} dk \omega_{j,k} a_{j,k}^\dagger a_{j,k} + \omega_a \sigma_+ \sigma_-, \quad (1)$$

and the dipole interaction,

$$V_r = \sum_j \int_{-\infty}^{+\infty} dk g_{j,k} (a_{j,k} \sigma_+ + a_{j,k}^\dagger \sigma_-), \quad (2)$$

$$V_d = \sum_j \int_{-\infty}^{+\infty} dk g_{j,k} (a_{j,k}^\dagger \sigma_+ + a_{j,k} \sigma_-), \quad (3)$$

with the atomic operator $\sigma_+ \equiv |e\rangle\langle g|$, $\sigma_- \equiv |g\rangle\langle e|$. Here, the mode-dependent coupling strength reads $g_{j,k} = -\sin \frac{m\pi}{2} \sin \frac{n\pi}{2} g \Omega_j / \sqrt{\omega_{j,k}}$, with $j \equiv (m, n)$, $g = d / \sqrt{\pi A}$. The matrix element d of the dipole transition is set to be real. Note that the coupling strength vanishes for even integer m or n . In this article, we focus on single-photon scattering in the weak-coupling regime, so that the rotating-wave approximation (RWA) can be used, $H = H_0 + V_r$, and the excitation number of the system is conserved. Details of the derivation of the Hamiltonian are given in the Appendix.

III. THE SCATTERING EQUATION

We now consider single-photon scattering in this hybrid system. For a single photon input in state $|\phi_{j,k}\rangle \equiv a_{j,k}^\dagger |\emptyset\rangle$ with energy $E = \omega_{j,k}$, the scattering state assumes the form

$$|\phi_{j,k}^{(+)}\rangle = \sum_{j'} \int dk' U_g(j', k'; j, k) a_{j',k'}^\dagger |\emptyset\rangle + U_e(j, k) \sigma_+ |\emptyset\rangle, \quad (4)$$

which ensures the conservation of the excitation number in the single-excitation subspace. Here, $|\emptyset\rangle$ represents the TLS in the ground state and the waveguide field in vacuum. The

scattering state is related to the input state via the Lippmann Schwinger equation,

$$|\phi_{j,k}^{(+)}\rangle = |\phi_{j,k}\rangle + \frac{1}{E - H_0 + i0^+} V_r |\phi_{j,k}^{(+)}\rangle. \quad (5)$$

By solving the Lippmann Schwinger equation, we obtain the amplitudes U_g and U_e as

$$U_e(j, k) = \frac{g_{j,k}}{E - \omega_a - \Delta(E) + i\Gamma(E)}, \quad (6)$$

$$U_g(j', k'; j, k) = \delta_{j',j} \delta(k' - k) + \frac{1}{E - \omega_{j',k'} + i0^+} g_{j',k'} U_e(j, k), \quad (7)$$

where the functions Δ and Γ are defined as

$$\Delta(E) = \sum_j \int_{-\infty}^{+\infty} dk \mathcal{P} \left(\frac{1}{E - \omega_{j,k}} \right) |g_{j,k}|^2, \quad (8)$$

$$\Gamma(E) = \pi \sum_j \int_{-\infty}^{+\infty} dk \delta(E - \omega_{j,k}) |g_{j,k}|^2. \quad (9)$$

The elements of the scattering matrix \hat{S} can be obtained from the scattering state as

$$\begin{aligned} \langle \phi_{j',k'} | \hat{S} | \phi_{j,k} \rangle &= \delta_{j,j'} \delta(k - k') - 2\pi i \delta(\omega_{j',k'} - \omega_{j,k}) \langle \phi_{j',k'} | V_r | \phi_{j,k}^{(+)} \rangle \\ &= \delta_{j,j'} \delta(k - k') - 2\pi i \delta(\omega_{j',k'} - \omega_{j,k}) \\ &\quad \times \frac{g_{j',k'} g_{j,k}}{E - \omega_a - \Delta(E) + i\Gamma(E)}, \end{aligned} \quad (10)$$

where $\rho_j(E) \equiv \frac{E}{\sqrt{E^2 - \Omega_j^2}}$ and $k_{j'}$ is fixed by $E = \omega_{j',k_{j'}}$; i.e., $k_{j'} = \sqrt{E^2 - \Omega_j^2}$. Note that $\Delta(E)$ is the Lamb shift induced by the waveguide modes and $\Gamma(E)$ is the decay rate of the TLS into the waveguide modes.

IV. SINGLE-CHANNEL SCATTERING AND ITS LOSS

It is known that a TLS acts as a quantum switch for single photons confined in a single-mode waveguide [6–9]. To keep a photon propagating in a single quantum channel, this realistic waveguide requires that (i) the cross section must be small enough that $\Omega_2 - \Omega_1$ is large enough and (ii) the energy of the input photon $\omega_{1,k}$ is below the cutoff frequency Ω_2 , i.e., $k < \sqrt{\Omega_2^2 - \Omega_1^2}$. Under these conditions, the input state is $|\phi_{\text{in}}\rangle = a_{1,k_1}^\dagger |\emptyset\rangle$ and the outgoing state $|\phi_{\text{out}}\rangle = \hat{S} |\phi_{\text{in}}\rangle$ is obtained as

$$|\phi_{\text{out}}\rangle = r a_{1,-k_1}^\dagger |\emptyset\rangle + (1 + r) a_{1,k_1}^\dagger |\emptyset\rangle, \quad (11)$$

where r is the reflection amplitude, given by

$$r = \frac{-i\Gamma(\omega_{1,k_1})}{\omega_{1,k_1} - \omega_a - \Delta(\omega_{1,k_1}) + i\Gamma(\omega_{1,k_1})}, \quad (12)$$

and the reflectance is $R = |r|^2$. The total reflection $R = 1$ occurs when the energy of the incident photon ω_{1,k_1} is resonant with the renormalized transition frequency of the TLS ω_A , which is $\omega_{1,k_1} = \omega_A \simeq \omega_a + \Delta(\omega_a)$ in the weak-coupling limit $g \rightarrow 0^+$. Note that in previous studies [6,8,9,22], the Lamb

shift $\Delta(\omega_a)$, which arises from the renormalization of the TLS's energy level, has been ignored due to the use of a linear or quadratic dispersion approximation.

This total reflection can be interpreted with Fano resonance with the asymmetry parameter $q = 0$ [20,21]. With the TLS coupled to the waveguide continuum, Fano interference occurs between the photon directly transmitted and the photon re-emitted by the TLS. When the photon energy is tuned to be on resonance with the renormalized TLS, the photon amplitudes from the two paths differ by a phase shift π , resulting in completely destructive interference of transmitted amplitudes.

If the photon energy is so high that the cross section of the waveguide is not small enough to confine it in the lowest mode, then the effects of higher modes should be taken into account. In the case $E \in (\Omega_2, \Omega_3)$, Eq. (9) is simplified as

$$\Gamma(E) = \Gamma_1(E) + \Gamma_2(E), \quad (13)$$

$$\Gamma_1(E) = 2\pi\rho_1(E)g_{1,k_1}g_{1,k_1}, \quad (14)$$

$$\Gamma_2(E) = 2\pi\rho_2(E)g_{2,k_2}g_{2,k_2}, \quad (15)$$

where $E = \omega_{1,k_1} = \omega_{2,k_2}$, $k_2 = \sqrt{E^2 - \Omega_2^2}$. The outgoing state becomes

$$|\phi_{\text{out}}\rangle = r_1 a_{1,-k_1}^\dagger |\emptyset\rangle + t_1 a_{1,k_1}^\dagger |\emptyset\rangle + r_2 a_{2,-k_2}^\dagger |\emptyset\rangle + t_2 a_{2,k_2}^\dagger |\emptyset\rangle, \quad (16)$$

where the reflection and transmission amplitudes are given by

$$r_1 = \frac{-i\Gamma_1(E)}{E - \omega_a - \Delta(E) + i\Gamma(E)}, \quad (17)$$

$$t_1 = \frac{E - \omega_a - \Delta(E) + i\Gamma_2(E)}{E - \omega_a - \Delta(E) + i\Gamma(E)}, \quad (18)$$

$$r_2 = \frac{-i2\pi\rho_2(E)g_{1,k_1}g_{2,k_2}}{E - \omega_a - \Delta(E) + i\Gamma(E)}, \quad (19)$$

$$t_2 = \frac{-i2\pi\rho_2(E)g_{1,k_1}g_{2,k_2}}{E - \omega_a - \Delta(E) + i\Gamma(E)}. \quad (20)$$

The reflectance and transmittance in the second mode are given by $R_2 = |r_2|^2\rho_1(E)/\rho_2(E)$ and $T_2 = |t_2|^2\rho_1(E)/\rho_2(E)$, respectively, while those in the first mode are given by $R_1 = |r_1|^2$ and $T_1 = |t_1|^2$. It is observed that the probability conservation $T_1 + R_1 + T_2 + R_2 = 1$ holds and the photon is partly lost into the higher mode. At the Fano resonance point $E = E_R$ [with $E_R - \omega_a - \Delta(E_R) = 0$], there are

$$R_1 = \left[\frac{\Gamma_1(E_R)}{\Gamma(E_R)} \right]^2, \quad (21)$$

$$R_2 = \frac{\Gamma_1(E_R)\Gamma_2(E_R)}{[\Gamma(E_R)]^2}, \quad (22)$$

and the total reflectance $R = R_1 + R_2 = \Gamma_1(E_R)/\Gamma(E_R) < 1$, implying no total reflection on Fano resonance. In the scattering process the photon is partly lost into higher modes, which cannot interfere due to mode mismatch, and consequently, the Fano resonance cannot induce total reflections.

In Fig. 2, we plot the reflectance $R = |r|^2$ as a function of the incident energy $E = \omega_{1,k}$. (with E is in units of π/a .) A single photon confined in the TM_{11} mode [see Fig. 2(a)] is indeed perfectly reflected by the TLS provided that ω_a is in the central domain of $[\Omega_1, \Omega_2]$. However, the position of the total reflection experiences a Lamb shift from ω_a due to the renormalization, which becomes larger as the coupling strength increases. It is observed that the total reflection also occurs when $E \rightarrow \Omega_1 + 0^+$, which is referred to as the cutoff frequency resonance [22], and its mechanism is due to the divergent decay rate $\Gamma(E) \rightarrow \infty$ caused by the divergence in the photon density of states. When the incident energy E is above Ω_2 , higher order modes and the induced multichannel interference effects must be taken into account. The reflectance with $E \in [\Omega_2, \Omega_3]$ is plotted in Fig. 2(b). Although ω_a still determines the reflection peak, the peak maximum becomes smaller than unity, showing that single photons in the TM_{11} mode experience a finite loss due to the existence of higher order modes in a realistic waveguide. Actually, this loss is caused by the TLS mediating the resonant tunneling process between the TM_{11} mode and higher order modes.

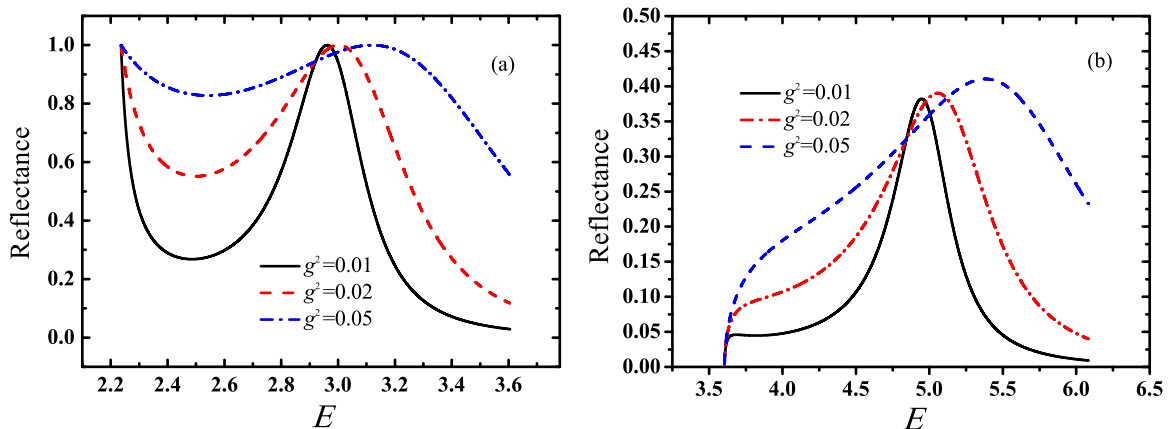


FIG. 2. (Color online) Reflectance spectrum for a single photon incident in the TM_{11} mode. (a) $E \in (\Omega_1, \Omega_2)$; $\omega_a = (\Omega_1 + \Omega_2)/2$. (b) $E \in (\Omega_2, \Omega_3)$; $\omega_a = (\Omega_2 + \Omega_3)/2$.

V. MULTICHANNEL SCATTERING AND THE CONTROLLABLE CHANNEL

As demonstrated in the preceding section, single photons with energy $E > \Omega_2$ cannot be well controlled due to loss into higher modes. However, as we show below, this problem can be overcome by the quantum interference between different transverse modes. In this section we study the quantum interference among different TM_{mn} modes. We assume that a single photon with energy E is incident in this superposition state,

$$|\phi_{\text{in}}\rangle = \sum_{j=1}^{j_{\text{max}}(E)} \varphi_j a_{j,k_j}^\dagger |\phi_{j,k_j}\rangle, \quad (23)$$

where $j_{\text{max}}(E)$ is the highest mode a photon with energy E can reach, fixed by the condition $\Omega_{j_{\text{max}}(E)} < E < \Omega_{j_{\text{max}}(E)+1}$. The complex coefficients φ_j (with $j = 1, 2, 3, \dots$) represent the amplitudes in the j th mode. Here, $k_j = \sqrt{E^2 - \Omega_j^2}$ ($j = 1, 2, 3, \dots$) takes the discrete values illustrated in Fig. 1(c), i.e., the crossing points between the horizontal line $\omega_{j,k} = E$ and the dispersion curves. With the scattering matrix elements in Eq. (10), the multichannel outgoing state $|\phi_{\text{out}}\rangle \equiv \hat{S}|\phi_{\text{in}}\rangle$ reads

$$|\phi_{\text{out}}\rangle = |\phi_{\text{in}}\rangle - 2\pi i \frac{\sum_{j'} \varphi_{j'} g_{j',k_{j'}}}{E - \omega_a - \Delta(E) + i\Gamma(E)} \times \sum_j g_{j,k_j} \rho_j(E) (a_{j,k_j}^\dagger + a_{j,-k_j}^\dagger) |\emptyset\rangle, \quad (24)$$

where $\rho_j(E) \equiv E/\sqrt{E^2 - \Omega_j^2}$ is the photon density of states in the j th mode. For a photon with energy E , the Hilbert space can be decomposed as the vector $\varphi^{(c)}$, which is proportional to the vector $\mathbf{g} \equiv (g_{1,k_1}, g_{2,k_2}, \dots, g_{j_{\text{max}},k_{j_{\text{max}}}})$, and the complementary subspace, which is spanned by the vectors $\varphi^{(F)}$ orthogonal to \mathbf{g} ; i.e., $\sum_{j=1}^{j_{\text{max}}(E)} g_{j,k_j} \varphi_j^{(F)} = 0$. It is easy to verify that single photons incident in states $\varphi^{(F)}$ will be freely transmitted. Thus, the vectors $\varphi^{(F)}$ define the SFCs, which are decoupled from the TLS and span the scattering-free subspace. This phenomenon is similar to the dark state of a three-level atom to support the electromagnetic induced transparency. Actually, the scattering-free state $|\varphi^{(F)}\rangle = \sum_{j=1}^{j_{\text{max}}(E)} \varphi_j^{(F)} |\phi_{j,k_j}\rangle$ (with photon energy E) can be understood as a multicomponent dark state as illustrated in Fig. 1(b). There exist multichannel transitions from $|g; j, k_j\rangle \equiv |\phi_{j,k_j}\rangle$ ($j = 1, 2, \dots, j_{\text{max}}$) to $|e\rangle$. The quantum interference among these transition channels results in the transparency of the TLS with respect to the incident photon and thus the incident photon is freely transmitted.

The remaining state vector orthogonal to the scattering-free subspace, defined by $\varphi_j^{(c)} \propto g_{j,k_j}$, can be well controlled by the TLS and thus we name it the CC. In the CC, the incident photon is scattered by the TLS into a superposition of transmitted and reflected waves, described by the outgoing state

$$|\phi_{\text{out}}\rangle = \sum_{j=1}^{j_{\text{max}}(E)} \varphi_j^{(c)} [t(E) a_{j,k_j}^\dagger + r(E) a_{j,-k_j}^\dagger] |\emptyset\rangle, \quad (25)$$

where $r(E)$ is the reflection amplitude, given by

$$r(E) = \frac{-i\Gamma(E)}{E - \omega_a - \Delta(E) + i\Gamma(E)}, \quad (26)$$

and $t(E)$ is the transmission amplitude, given by $t(E) = 1 + r(E)$.

It is observed from Eq. (25) that both the transmitted and the reflected photons remain in the transverse state $\varphi_j^{(c)}$ of the incident photon. The probability conservation $|r(E)|^2 + |t(E)|^2 = 1$ holds for each transverse mode, implying that the photon never transfers from one mode to the other in elastic scattering. It follows from Eq. (26) that the scattering of a single photon in the CC exhibits the same features as that in the single-mode model [see Eq. (12)]. Total reflection occurs on Fano resonance, with the energy E_R fixed by the equation $[E - \omega_a - \Delta(E)]_{E=E_R} = 0$. Besides, total reflections also occur whenever $E \rightarrow \Omega_j + 0^+$ ($j = 1, 2, 3, \dots$), since at the band edge the divergence in the photon density of states causes $\Gamma(E) \rightarrow \infty$.

It is well known that when the cross section of the waveguide becomes larger or the frequency of the incident photon becomes higher, the photon will be transmitted more easily. This is because while the dimension of the scattering-free subspace increases, that of the CC remains only 1. In spite of this, we can always make the photon totally reflected provided it is precisely prepared in the unique CC. As inferred from Eq. (24), the spontaneous emission of the TLS is in the CC. Thus, the initial state of the photon can be prepared in the CC by another excited TLS, which is coupled to the waveguide. We can direct the spontaneously emitted photons along the waveguide to act as incident photons.

The reflectance spectrum for a single photon incident in the CC and that in the TM_{11} mode are compared in Fig. 3(a). For a single photon incident in the TM_{11} mode, the loss into higher order modes mediated by the TLS cannot interfere with the incident wave due to mode mismatch. As a result, the transmitted wave can never be completely canceled by Fano interference and thus the reflection peak on Fano resonance is less than unity. For the single photon incident in the CC, the photon loss into each mode from the other modes is exactly canceled and thus actually no photon transfers from one mode to another. In consequence, the single photons guided in the CC can be as well controlled by the TLS as in the single-mode model, as shown in Fig. 3(b). Note that the position of the total reflection is also shifted from the atomic transition frequency due to the Lamb shift.

For a finite waveguide-TLS coupling which is in the weak-coupling regime, the Fano resonance energy should be determined by solving the transcendental equation $[E - \omega_a - \Delta(E)]_{E=E_R} = 0$, which may have more than one solution, rather than the single solution $E_R = \omega_A \simeq \omega_a + \Delta(\omega_a)$ in the weak-coupling limit $g \rightarrow 0^+$. Here, we consider the contribution of several low modes to the Lamb shift and a precise calculation shall be presented elsewhere. With the inclusion of more modes, multi-peaks are observed in the reflectance spectrum as illustrated in Fig. 4. The additional emergent peaks are cutoff frequency resonances.

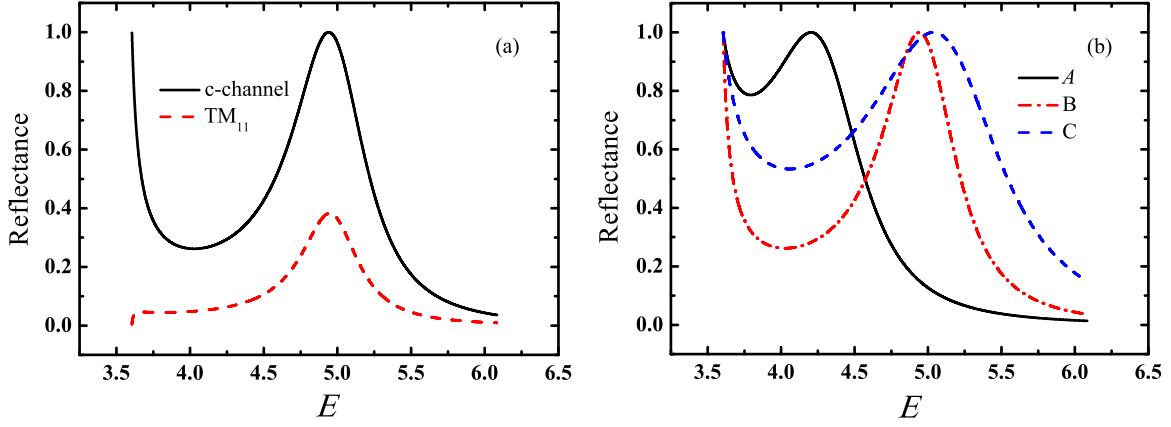


FIG. 3. (Color online) (a) Reflectance spectrum with $E \in (\Omega_2, \Omega_3)$. A single photon is input in TM₁₁ [dashed (red) line] or input in the CC (solid black line). $g^2 = 0.01$; $\omega_a = (\Omega_2 + \Omega_3)/2$. (b) Reflectance spectrum with $E \in (\Omega_2, \Omega_3)$ for a single photon input in the CC. (A) $\omega_a = 0.8\Omega_2 + 0.2\Omega_3$, $g^2 = 0.01$; (B) $\omega_a = 0.5(\Omega_2 + \Omega_3)$, $g^2 = 0.01$; (C) $\omega_a = 0.5(\Omega_2 + \Omega_3)$, $g^2 = 0.02$.

VI. THE COUNTER-ROTATING INTERACTION

To explore the effects of counter-rotating terms which violate the excitation-number conservation, we carry out a perturbative calculation based on the RWA result by treating V_d as a perturbation. The scattering state with the first-order correction of V_d is obtained as

$$|\tilde{\phi}_{j,k}^{(+)}\rangle = |\phi_{j,k}^{(+)}\rangle + \frac{1}{\omega_{j,k} - \hat{H}_0 + i0^+} V_d |\phi_{j,k}^{(+)}\rangle, \quad (27)$$

where $|\phi_{j,k}^{(+)}\rangle$ is the scattering state in the RWA as shown in Eq. (4) and the second term is the correction contributed by the three-excitation process. Accordingly, the scattering matrix element is obtained as

$$\langle \phi_{j',k'} | \hat{S} | \phi_{j,k} \rangle = \langle \phi_{j',k'} | \phi_{j,k} \rangle - 2\pi i \delta(\omega_{j',k'} - \omega_{j,k}) \langle \phi_{j',k'} | V | \tilde{\phi}_{j,k}^{(+)} \rangle. \quad (28)$$

Using Eq. (27) in Eq. (28) we obtain the first-order correction to the scattering matrix element as $-2\pi i \delta(\omega_{j',k'} - \omega_{j,k}) T_1(\phi_{j',k'} \leftarrow \phi_{j,k})$,

$$T_1(\phi_{j',k'} \leftarrow \phi_{j,k}) = \frac{g_{j',k'} g_{j,k} [-F(\omega_{j,k})]}{\omega_{j,k} - \omega_a - \Delta(\omega_{j,k}) + i\Gamma(\omega_{j,k})}, \quad (29)$$

where

$$F(\omega_{j,k}) \equiv \frac{\omega_{j,k} - \omega_a + \Delta_a}{\omega_{j,k} + \omega_a}, \quad (30)$$

$$\Gamma(\omega_{j,k}) \equiv \pi \sum_{j_1} \int dk_1 |g_{j_1,k_1}|^2 \delta(\omega_{j,k} - \omega_{j_1,k_1}), \quad (31)$$

$$\Delta_a \equiv \sum_{j_1} \int dk_1 |g_{j_1,k_1}|^2 \frac{1}{\omega_{j_1,k_1} + \omega_a}. \quad (32)$$

Note that the term $2\pi i \delta(\omega_{j',k'} - \omega_{j,k}) U_g(j',k'; j,k) \sum_{j_2} \int dk_2 g_{j_2,k_2}^2 / (\omega_{j_2,k_2} + \omega_a)$ contributed by the ‘‘vacuum bubble diagrams’’ is discarded [23,24]. Thus, the scattering matrix element incorporating the first-order effects of the counter-rotating interaction is given by

$$\begin{aligned} \langle \phi_{j',k'} | \hat{S} | \phi_{j,k} \rangle &= \delta_{j,j'} \delta(k - k') - 2\pi i \delta(\omega_{j',k'} - \omega_{j,k}) [1 - F(\omega_{j,k})] \\ &\times \frac{g_{j',k'} g_{j,k}}{\omega_{j,k} - \omega_a - \Delta(\omega_{j,k}) + i\Gamma(\omega_{j,k})}. \end{aligned} \quad (33)$$

It is inferred from Eq. (33) that the counter-rotating terms will not change the multichannel interference phenomena, since

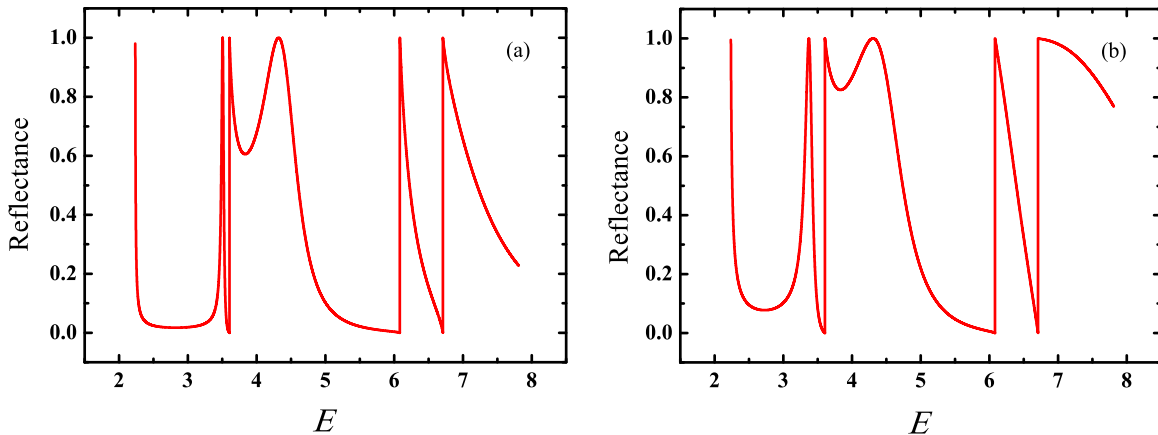


FIG. 4. (Color online) Reflectance spectrum with $E \in (\Omega_1, \Omega_5)$ for a single photon input in the CC. (a) $g^2 = 0.01$; $\omega_a = (\Omega_1 + \Omega_5)/2$. (b) $g^2 = 0.0$; $\omega_a = (\Omega_2 + \Omega_5)/2$.

the only effect is a quantitative modulation of the reflection amplitude. In the CC, the reflection amplitude becomes

$$r(E) = \frac{-i\Gamma(E)[1 - F(E)]}{E - \omega_a - \Delta(E) + i\Gamma(E)}. \quad (34)$$

In the regime $E \gg \omega_a$, $1 - F(E) \simeq 0$, $r(E) \simeq 0$, implying that multi-peaks at the cutoff frequency of each transverse mode (see Fig. 4) would be lowered or even removed. In comparison with the RWA result, the reflection amplitude with the first-order counter-rotating correction is modulated by the function $1 - F(E)$, which implies that the multi-peaks in the off-resonant regime will be lower and even removed due to the counter-rotating interaction.

VII. CONCLUSIONS

In a realistic waveguide of a rectangular cross section, the TLS embedded acts as a quantum switch for single photons with energy $E \in (\Omega_1, \Omega_2)$. At a higher energy, $E \in (\Omega_2, \infty)$, single photons incident in TM₁₁ will be "lost" into higher order modes via the TLS, resulting in the breakdown of the quantum switch. Fortunately, by guiding single photons into the CC instead of TM₁₁, the quantum switch can be restored due to multichannel quantum interference.

For an artificial atom of transition frequency $\omega_A \simeq 10.2$ GHz [25] to work as a quantum switch, the cutoff frequencies of the waveguide should satisfy $(\Omega_1 + \Omega_2)/2 \simeq \omega_A$, leading to the cross section $a/2 = b \simeq 2.1$ cm. Correspondingly, $\Omega_2 \simeq 79.1$ GHz, so that the scattering of microwave photons with energy $E \gtrsim 79.1$ GHz cannot be confined in TM₁₁ and multichannel effects (loss and interference) are thus involved. In order to control photons with a higher energy, e.g., $\omega_A \simeq 1000$ GHz, we should use a waveguide of size $a/2 = b \simeq 2.1$ μm to work in the single-mode region; otherwise, if $b > 2.7$ μm , i.e., $\Omega_2 < 1000$ GHz, the waveguide will work in the multichannel region. Consequently, we should utilize the CC scheme to overcome the channel loss. The existence of the unique TLS CC and the complementary SFCs guarantees success in controlling single photons in the realistic waveguide of a finite cross section.

For physical implementation of the waveguide-QED system, apart from the metallic rectangular waveguide considered here, other architectures, such as a defect waveguide in a 3D (or 2D) photonic crystal coupled to a quantum dot [26,27], an optical fiber with a TLA embedded, or an x-ray waveguide [28] with a localized nucleon, can also be used. Actually, the multichannel interference phenomena found here can be displayed in any Fano interference model in which the continuum of propagation modes is degenerate (the guiding modes here are degenerate labeled by transverse modes).

ACKNOWLEDGMENTS

We are grateful to C. Y. Cai, T. Tian, J. F. Huang, Y. Li, P. Zhang and D. Z. Xu for helpful discussions. This work was supported by National Natural Science Foundation of China under Grants No. 11121403, No. 10935010, No. 11222430, No. 11074305, No. 11074261 and National 973 program (Grants No. 2012CB922104 and No. 2014CB921402).

APPENDIX

The quantization of the waveguide field is based on the classical Maxwell equations with the boundary condition of metallic rectangular waveguides. The electric field can be expanded by the mode functions as

$$\mathbf{E}(\mathbf{r}, t) = i \sum_{\lambda=1,2} \sum_{\mathbf{k}} \sqrt{\frac{1}{2}} \omega_{\mathbf{k}} (c_{\mathbf{k},\lambda}(t) \mathbf{u}_{\mathbf{k},\lambda}(\mathbf{r}) - c_{\mathbf{k},\lambda}^*(t) \mathbf{u}_{\mathbf{k},\lambda}^*(\mathbf{r})), \quad (A1)$$

with $\mathbf{k} \equiv (\mathbf{k}_x, \mathbf{k}_y, k)$. The Maxwell equation of the electric field reads $(\nabla^2 - \frac{\partial^2}{\partial t^2})\mathbf{E}(\mathbf{r}, t) = 0$, and thus the mode functions obey the wave equation $(\nabla^2 + \omega_{\mathbf{k}}^2)\mathbf{u}_{\mathbf{k},\lambda}(\mathbf{r}) = 0$ with $c_{\mathbf{k},\lambda}(t) = c_{\mathbf{k},\lambda} e^{-i\omega_{\mathbf{k}} t}$. With the boundary condition of metallic rectangular waveguides, the wave equation gives the mode functions as

$$\mathbf{u}_{\mathbf{k},\lambda}^{(x)}(\mathbf{r}) = \mathbf{C}_{\mathbf{k},\lambda}^{(x)} \cos(k_x x) \sin(k_y y) e^{ikz}, \quad (A2)$$

$$\mathbf{u}_{\mathbf{k},\lambda}^{(y)}(\mathbf{r}) = \mathbf{C}_{\mathbf{k},\lambda}^{(y)} \sin(k_x x) \cos(k_y y) e^{ikz}, \quad (A3)$$

$$\mathbf{u}_{\mathbf{k},\lambda}^{(z)}(\mathbf{r}) = \mathbf{C}_{\mathbf{k},\lambda}^{(z)} \sin(k_x x) \sin(k_y y) e^{ikz}, \quad (A4)$$

where $k_x = \frac{m\pi}{a}$, $k_y = \frac{n\pi}{b}$, m and n are non-negative integers, $\omega_{\mathbf{k}} = \sqrt{\Omega_{m,n}^2 + k^2}$, $\Omega_{m,n} = \sqrt{k_x^2 + k_y^2}$, and $\mathbf{C}_{\mathbf{k},\lambda}^{(x,y,z)}$ is the normalization constant. In addition, the Maxwell equations require $\nabla \cdot \mathbf{E} = 0$, which means $k_x \mathbf{C}_{\mathbf{k},\lambda}^{(x)} + k_y \mathbf{C}_{\mathbf{k},\lambda}^{(y)} - ik \mathbf{C}_{\mathbf{k},\lambda}^{(z)} = 0$. Therefore, there are two mode functions, reading

$$\mathbf{u}_{\mathbf{k},1}(\mathbf{r}) = \frac{2}{\sqrt{2\pi A}} \frac{1}{\Omega_{m,n}} \left[\frac{n\pi}{b} \cos\left(\frac{m\pi}{a}x\right) \sin\left(\frac{n\pi}{b}y\right) e^{ikz} \mathbf{e}_x - \frac{m\pi}{a} \sin\left(\frac{m\pi}{a}x\right) \cos\left(\frac{n\pi}{b}y\right) e^{ikz} \mathbf{e}_y \right], \quad (A5)$$

$$\mathbf{u}_{\mathbf{k},2}(\mathbf{r}) = \frac{2}{\sqrt{2\pi A}} \frac{1}{\Omega_{m,n}} \frac{k}{\omega_{\mathbf{k}}} \left[\frac{m\pi}{a} \cos\left(\frac{m\pi}{a}x\right) \sin\left(\frac{n\pi}{b}y\right) \times e^{ikz} \mathbf{e}_x + \frac{n\pi}{b} \sin\left(\frac{m\pi}{a}x\right) \cos\left(\frac{n\pi}{b}y\right) e^{ikz} \mathbf{e}_y - i \frac{1}{k} \Omega_{m,n}^2 \sin\left(\frac{m\pi}{a}x\right) \sin\left(\frac{n\pi}{b}y\right) e^{ikz} \mathbf{e}_z \right]. \quad (A6)$$

The magnetic field is obtained from the electric field via $\partial \mathbf{B} / \partial t = -\nabla \times \mathbf{E}$. It is easy to verify that $\mathbf{u}_{\mathbf{k},1}(\mathbf{r})$ is the TE mode function and $\mathbf{u}_{\mathbf{k},2}(\mathbf{r})$ is the TM mode function. The total energy of the waveguide field is

$$\begin{aligned} \mathcal{E} &= \frac{1}{2} \int d\mathbf{r} (\mathbf{E} \cdot \mathbf{E} + \mathbf{B} \cdot \mathbf{B}) \\ &= \sum_{\lambda=1,2} \sum_{\mathbf{k}} \frac{1}{2} \omega_{\mathbf{k}} (c_{\mathbf{k},\lambda}^* c_{\mathbf{k},\lambda} + c_{\mathbf{k},\lambda} c_{\mathbf{k},\lambda}^*). \end{aligned} \quad (A7)$$

The quantization is carried out by promoting the expansion coefficients to operators,

$$\begin{aligned} c_{\mathbf{k},\lambda} &\rightarrow \hat{c}_{\mathbf{k},\lambda}, \\ c_{\mathbf{k},\lambda}^* &\rightarrow \hat{c}_{\mathbf{k},\lambda}^\dagger, \end{aligned}$$

which obey the commutation relations

$$\begin{aligned} [\hat{c}_{\mathbf{k},\lambda}, \hat{c}_{\mathbf{k}',\lambda'}^\dagger] &= \delta_{\lambda,\lambda'} \delta_{\mathbf{k},\mathbf{k}'} \delta(k - k'), \\ [\hat{c}_{\mathbf{k},\lambda}, \hat{c}_{\mathbf{k}',\lambda'}] &= 0, \\ [\hat{c}_{\mathbf{k},\lambda}^\dagger, \hat{c}_{\mathbf{k}',\lambda'}^\dagger] &= 0. \end{aligned}$$

Thus, the Hamiltonian of the waveguide field is

$$\hat{H}_w = \sum_{\lambda=1,2} \sum_{\mathbf{k}} \omega_{\mathbf{k}} \left(\hat{c}_{\mathbf{k},\lambda}^\dagger \hat{c}_{\mathbf{k},\lambda} + \frac{1}{2} \right). \quad (\text{A8})$$

Hereafter we neglect the hat on operators. The dipole of the TLS oriented along the z direction is only coupled to the TM modes. The TM field alone is described by

$$H_w = \sum_{\mathbf{k}} \omega_{\mathbf{k}} \left(c_{\mathbf{k}}^\dagger c_{\mathbf{k}} + \frac{1}{2} \right). \quad (\text{A9})$$

The dipole coupling of the TLS to the TM field is given by $-\mathbf{d} \cdot \mathbf{E}(\mathbf{r}_a)$, where \mathbf{d} is the dipole of the TLS and \mathbf{r}_a is

the location of the TLS. With $\mathbf{r}_a = (a/2, b/2, 0)$, the dipole interaction reads

$$V = \sum_j \int_{-\infty}^{+\infty} dk g_{j,k} (a_{j,k}^\dagger + a_{j,k}) (\sigma_+ + \sigma_-), \quad (\text{A10})$$

where $j \equiv (m, n)$, $\mathbf{k} \equiv (m, n, k) \equiv (j, k)$, $a_{j,k} \equiv c_{\mathbf{k}}$, σ_+ (σ_-) is the transition operator of the TLS, and the coupling coefficient $g_{j,k}$ is given by

$$g_{j,k} = -\frac{d}{\sqrt{\pi A}} \frac{\Omega_j}{\sqrt{\omega_{j,k}}} \sin\left(\frac{m\pi}{2}\right) \sin\left(\frac{n\pi}{2}\right). \quad (\text{A11})$$

Here, $\omega_{j,k} = \sqrt{\Omega_j^2 + k^2}$, $d = \langle e | \mathbf{d} | g \rangle \cdot \mathbf{e}_z$, and d is set to be real. Note that $g_{j,k} = 0$ for even integer m or n . The TM_{mn} mode (with odd integers m and n) is labeled by the sequence number j according to the ascending order of the cutoff frequencies, or more specifically, $1 \equiv (1, 1)$, $2 \equiv (3, 1)$, $3 \equiv (1, 3)$, $4 \equiv (3, 3)$, etc.

-
- [1] S. E. Harris and Y. Yamamoto, *Phys. Rev. Lett.* **81**, 3611 (1998).
[2] B. S. Ham and P. R. Hemmer, *Phys. Rev. Lett.* **84**, 4080 (2000).
[3] K. M. Birnbaum *et al.*, *Nature (London)* **436**, 87 (2005).
[4] M. Bajcsy, S. Hofferberth, V. Balic, T. Peyronel, M. Hafezi, A. S. Zibrov, V. Vuletic, and M. D. Lukin, *Phys. Rev. Lett.* **102**, 203902 (2009).
[5] S. C. Zhang, C. Liu, S. Y. Zhou, C. S. Chuu, M. M. T. Loy, and S. W. Du, *Phys. Rev. Lett.* **109**, 263601 (2012).
[6] J. T. Shen and S. Fan, *Phys. Rev. Lett.* **95**, 213001 (2005); **98**, 153003 (2007); *Opt. Lett.* **30**, 2001 (2005).
[7] L. Zhou, Z. R. Gong, Y. X. Liu, C. P. Sun, and F. Nori, *Phys. Rev. Lett.* **101**, 100501 (2008); L. Zhou, L. P. Yang, Y. Li, and C. P. Sun, *ibid.* **111**, 103604 (2013).
[8] T. Shi and C. P. Sun, *Phys. Rev. B* **79**, 205111 (2009).
[9] T. S. Tsoi and C. K. Law, *Phys. Rev. A* **78**, 063832 (2008); **80**, 033823 (2009).
[10] X. Zang and C. Jiang, *J. Phys. B* **43**, 215501 (2010).
[11] T. Aoki, A. S. Parkins, D. J. Alton, C. A. Regal, B. Dayan, E. Ostby, K. J. Vahala, and H. J. Kimble, *Phys. Rev. Lett.* **102**, 083601 (2009).
[12] D. E. Chang, A. S. Sørensen, E. A. Demler, and M. D. Lukin, *Nat. Phys.* **3**, 807 (2007).
[13] J. Hwang *et al.*, *Nature* **460**, 76 (2009).
[14] A. Wallraff *et al.*, *Nature (London)* **431**, 162 (2004).
[15] J. Q. You and F. Nori, *Phys. Today* **58**, 42 (2005).
[16] K. LeHur, *Phys. Rev. B* **85**, 140506(R) (2012).
[17] M. Goldstein, M. H. Devoret, M. Houzet, and L. I. Glazman, *Phys. Rev. Lett.* **110**, 017002 (2013).
[18] D. J. Egger and F. K. Wilhelm, *Phys. Rev. Lett.* **111**, 163601 (2013).
[19] H. Zheng, D. J. Gauthier, and H. U. Baranger, *Phys. Rev. A* **82**, 063816 (2010); *Phys. Rev. Lett.* **111**, 090502 (2013).
[20] U. Fano, *Phys. Rev.* **124**, 1866 (1961).
[21] A. E. Miroshnichenko, S. Flach, and Y. S. Kivshar, *Rev. Mod. Phys.* **82**, 2257 (2010).
[22] J. F. Huang, T. Shi, C. P. Sun, and F. Nori, *Phys. Rev. A* **88**, 013836 (2013).
[23] M. E. Peskin and D. V. Schroeder, *An Introduction to Quantum Field Theory* (Westview Press, Boulder, CO, 1995).
[24] A. L. Fetter and J. D. Walecka, *Quantum Theory of Many Particle Systems* (McGraw-Hill, New York, 1971).
[25] O. Astafiev *et al.*, *Science* **327**, 840 (2010).
[26] S. O. Konorov *et al.*, *JETP Lett.* **76**, 341 (2002).
[27] S. Hughes, *Opt. Lett.* **29**, 2659 (2004); S. Hughes and H. Kamada, *Phys. Rev. B* **70**, 195313 (2004).
[28] K. Okamoto, T. Noma, A. Komoto, W. Kubo, M. Takahashi, A. Iida, and H. Miyata, *Phys. Rev. Lett.* **109**, 233907 (2012).